Field Emission and Particle Sensing Devices Based on Arrayed Carbon Nanotubes and Related Nanostructures for Defense Applications

AOARD 044063

Li-Chyong Chen
National Taiwan University

April 2007

Report Documentation Page

Form Approved
OMB No. 0704-0188

1. REPORT DATE	2. REPORT TYPE	3. DATES COVERED
31 OCT 2008		

4. TITLE AND SUBTITLE	5a. CONTRACT NUMBER
Field Emission and Particle Sensing Devices Based on Arrayed Carbon Nanotubes and Related Nanostructures for Defense Applications	**FA520905P0362**
	5b. GRANT NUMBER
	5c. PROGRAM ELEMENT NUMBER
6. AUTHOR(S)	5d. PROJECT NUMBER
Li-Chyong Chen	5e. TASK NUMBER
	5f. WORK UNIT NUMBER
7. PERFORMING ORGANIZATION NAME(S) AND ADDRESS(ES)	8. PERFORMING ORGANIZATION REPORT NUMBER
National Taiwan University,1 Roosevelt Road. Section 4,Taipei,Taiwan,NA,106	**N/A**
9. SPONSORING/MONITORING AGENCY NAME(S) AND ADDRESS(ES)	10. SPONSOR/MONITOR'S ACRONYM(S)
	11. SPONSOR/MONITOR'S REPORT NUMBER(S)

12. DISTRIBUTION/AVAILABILITY STATEMENT

Approved for public release; distribution unlimited.

13. SUPPLEMENTARY NOTES

14. ABSTRACT

This project covered efforts to develop and test the field-emission and particle sensing devices (FED and PSD) using carbon nanotubes (CNTs), and SiC capped Si nanotips (SiNTs) arrays. Additional studies focused on tungsten nanotips. The report covers successes on all efforts, including structural characterization and tip performance.

15. SUBJECT TERMS

16. SECURITY CLASSIFICATION OF:			17. LIMITATION OF ABSTRACT	18. NUMBER OF PAGES	19a. NAME OF RESPONSIBLE PERSON
a. REPORT	b. ABSTRACT	c. THIS PAGE			
unclassified	**unclassified**	**unclassified**		**22**	

Field Emission and Particle Sensing Devices Based on Arrayed Carbon Nanotubes and Related Nanostructures for Defense Applications

Main PI:

Dr. Li-Chyong Chen, Research Fellow

Center for Condensed Matter Sciences, National Taiwan University

1, Roosevelt Road, Section 4, Taipei 106, Taiwan

Tel: 886-2-3366-5249; Fax: 886-2-2365-5404

E-mail:chenlc@ntu.etdu.tw

Co-PI:

Dr. Kuei-Hsien Chen, Research Fellow

Institute of Atomic and Molecular Sciences, Academia Sinica

PO Box 23-166, Taipei 106, Taiwan

Tel: 886-2-2366-8232; Fax: 886-2-2362-0200

E-mail:chenkh@pub.iams.sinica.edu.tw

Abstract

We report two types of sensors, namely, carbon nanotubes (CNTs) field emission gas sensors and silicon nanotips (SiNTs) based molecule sensors. On-chip wafer processes have been applied to fabricate the vertically aligned, high-density arrays of CNTs and SiNTs. Field emission behavior of CNTs is strongly dependent on the vacuum condition and ambient gaseous species, thus they can be functioning as field emission gas sensors. SiNTs arrays with a tip density as high as 10^{12} cm^{-2} have been fabricated and when dispersed with Ag nanoparticles (NPs) of optimized size and inter-particle distance, they show excellent surface enhanced Raman effect (up to 8-order enhancement), suggesting potential application of Ag NPs-dispersed nanotip arrays as molecular sensors. The wetting properties of SiNTs are also discussed. Water contact angles were measured as a function of their aspect ratio (α) and the inter-tip distance. The hydrophilic nature of the SiNTs is tunable with α and the inter-tip distance. Super-hydrophilicity was observed with $\alpha > 12$ (length ~ 1500 nm). Upon coating with TiO_2, a switchover from super-hydrophilic to hydrophobic surface properties has been observed.

Introduction

During the past few years, our laboratory has accumulated substantial experience to fabricate carbon nanotubes (CNTs) with reasonably good control by microwave plasma enhanced chemical vapor deposition (MPECVD) [1]. The MPECVD process not only produces phase-pure CNTs with high uniformity but also makes direct growth on selective area possible in the same time. Most remarkably, an on-chip process has been established to control the emitter site density in a cost-effective manner [2]. Prototypes of CNTs-based field emission devices (FEDs), including diode-type, triode-type, gate controlled and thin-film-transistor (TFT) controlled, have been demonstrated [3-8]. Besides conventional vertical design, lateral emission devices have also been fabricated recently by our group [9]. Inspired by the fact that field emission behavior is strongly dependent on the vacuum condition and ambient gaseous species, we have explored the feasibility of using CNTs as field emission gas sensors.

Up until now, a large number of gas sensors based on CNTs have been demonstrated, which can be categorized by the following three major techniques: electrical transport, microbalance and gas ionization [10-13]. The electrical method has extremely high sensitivity but is limited by several factors, such as the inability to identify gases with low adsorption energies, poor diffusion kinetics or poor charge transfer with nanotubes. Quartz crystal microbalance (QCM) can also be effective for gas detection down to about 10^{-9} g (giving a change in QCM frequency of ±1 Hz) but its lack of chemical specificity and/or adsorption efficiency of specific gas of interest can be problematic. Ionization sensors work by fingerprinting the ionization characteristics of distinct gases, but its operation may involve risky high voltage. Here we propose CNTs-based field emission as an alternative method, in particular, when the sensing enviroment is high vacuum, including sensing device stationed in space vehicle.

Meanwhile, detection of gaseous molecules, either neutral or ionized, by optical tools such as surface enhanced Raman spectroscopy (SERS) is by no means an easy job when the detection is strongly limited by the adsorption of the gaseous molecules on the metal nanoparticles. These metal nanoparticles, with proper control in the inter-particle distance, are responsible for enhancing the weak Raman signals by way of dipole-dipole interaction. A simple scheme to increase the total number of “hotspots” is desired to

realize high-performance sensing *via* SERS. We have demonstrated high-density arrays of CNTs, Si nanotips and AlN nanorods to be excellent supports for self-assembly of Au and Ag nanoparticles, which are extremely effective in SERS [14-15]. Nanoscale engineering of surface, including the size, density and inter-particle distance of the metal nanoparticles has been established for optimized enhancement in SERS.

The emerging need for adequate hydrophobic properties is obvious because of the growing importance of bio-electromechanical systems where fluidic reactants are pushed through micrometer sized channels and reactions made to occur therein. Similar need is also expected for the thruster fuel injectors for space vehicles and some energetic electrochemical fuel cells for publics in general. It is known that a high degree of surface roughness (geometrical factor) results in solid surfaces having hydrophobic properties. A super-hydrophobic surface is created when such surface is coupled with a layer of low surface energy fluorinated compounds (chemical factor). Hydrophilic surfaces, on the other hand, are generated mostly by using dry processes such as corona discharge or a plasma discharge/jet on metal–polymer or metal–metal surfaces to enhance the adhesion and wettability. However, dynamic or reversible wetting–dewetting behavior seems to be the most attractive of the surface properties. We have studied the wetting properties of silicon nanotips (SiNTs) with both geometrical and chemical effects [16]. Unlike the usual monotonic change in the wetting behavior, we demonstrate a geometrically tunable hydrophilicity and a chemically modified switchover to hydrophobicity in the SiNTs.

Experimental

(1)Processes and Materials:

The main process techniques employed in the present project is MPECVD and electron-cyclotron-resonance plasma (ECR) process. The MPECVD process routines that give desired attributes of CNTs have been well-established, especially for Fe-catalyzed growth and device fabrication on Si substrate [1]. The ECR processes were carried out in gas mixtures of silane, methane, argon and hydrogen. The combination of chemical deposition and etching along with physical etching provides a unique way to fabricate high-density nanotips over a large area and a wide range of materials [17-18]. Using arrayed Si nanotips produced by ECR, subsequent deposition of Ag nanoparticles was

performed by ion-beam sputtering (IBS). The sputtered silver was collected on the substrate, kept at room temperature and a working pressure of about 5×10^{-4} Torr, for different durations of time. Replacing Ag target by TiO_2, the same technique was also applied to deposit TiO_2 nanoparticles onto SiNTs. Commonly used molecules for SERS experiments such as Rhodamine 6G and *trans*-1,2-bis(4-pyridyl)ethylene (BPE) (TCI, Tokyo, Japan) were then dispersed by drop coating onto these substrates, in measured quantities, from their solution (in methanol) and dried.

(2) Characterizations and Properties:

Field emission measurements were performed in a vacuum chamber at room temperature with controllable operating pressure and inlet gaseous species such as Ar, N_2, O_2, and NH_3 in measured amounts with the help of a mass flow controller. The anode-to-cathode distance was kept at 70 μm. Raman measurements were carried out using a Renishaw-2000 micro Raman spectroscope. Single accumulations with integration times of 5 seconds were used to collect the spectra in a backscattered mode. A 532-nm laser with a source intensity of 100 mW was used with a probe beam diameter of 1 μm. Different concentrations (10^{-6} to 10^{-10} M) of Rhodamine 6G and BPE were used and their Raman spectra were taken on these specialized substrates. The water contact angles were measured in a standard FACE contact anglemeter setup (model CA-D, Kyowa Interface Science Co. Ltd, Japan) attached to a CCD camera.

Results and Discussion

(1) Miniaturized field emission gas sensors using carbon nanotubes

The CNTs arrays grown Si substrate were vertically aligned with a typical tube diameter of 15 nm and a length of 10 μm, as shown in Figure 1(a). Figure 1(b) shows the field emission characteristics for our CNTs samples used in the present project. The base pressure of the vacuum chamber was kept at 8×10^{-7} Torr. The turn-on field, defined as the field at which a current density of 10 $\mu A/cm^2$ is emitted, was around 2.3 V/μm. With increasing applied voltage, the emission current increases sharply.

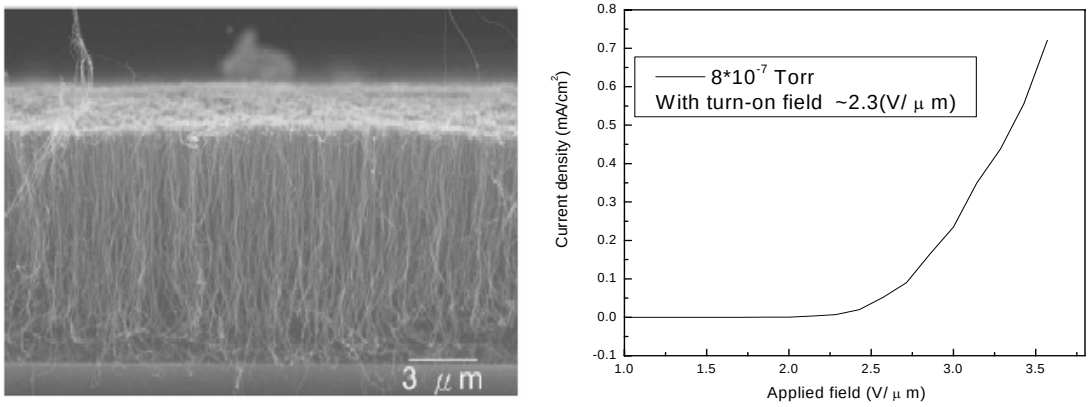

(a) (b)

Figure 1 (a) FESEM micrograph of the CNTs prepared by MWECVD showing the multi-wall CNTs are vertically aligned on Si substrate. (b) Typical field emission I-V curve showing a turn-on field of 2.3 V/μm.

Introducing any gas into the vacuum chamber and keeping it at a higher working pressure would change the emission current, of which the amount is dependent on the gas environment. Adsorption of molecules induces a charge transfer and determines the direction of the dipole field at the CNT edges. Usually, charges are transferred from the adsorbates to the CNT edges for hydrogen and water adsorptions, whereas the direction is reversed for nitrogen and oxygen adsorptions. Figure 2 shows the comparative study of steady-state field emission current measured in nitrogen and argon gases operated at four different levels of working pressure. The initial emission current measured at 1×10^{-6} Torr of nitrogen is quite similar to that of argon. However, as the working pressure was increased to 1×10^{-4} Torr, more pronounced reduction in the emission current was observed in nitrogen, compared to that in argon. This can be understood from the charge transfer view point. Presumably, nitrogen induced a dipole field whereas argon did not.

To check the reproducibility of field emission sensor, dynamic field emission measurements have been performed under varying pressures. Such measurements also allow us to study the response and recovery time after exposing to analyte gas and pumping back to background pressure, respectively. In general, the higher the working

pressure, the faster the response/recovering. As shown in Figure 3, CNTs field emitters exposed to nitrogen showed a slower response and recovery than those to argon.

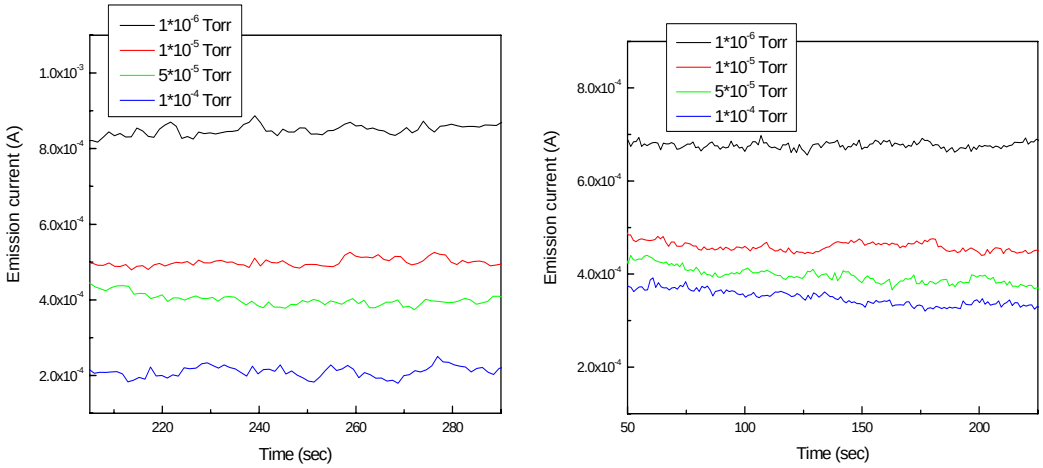

(a) (b)

Figure 2 Steady-state field emission currents of CNTs measured at four different operating pressures under (a) nitrogen and (b) argon at a constant voltage of 350 V, i.e., an effective field of 5 V/μm.

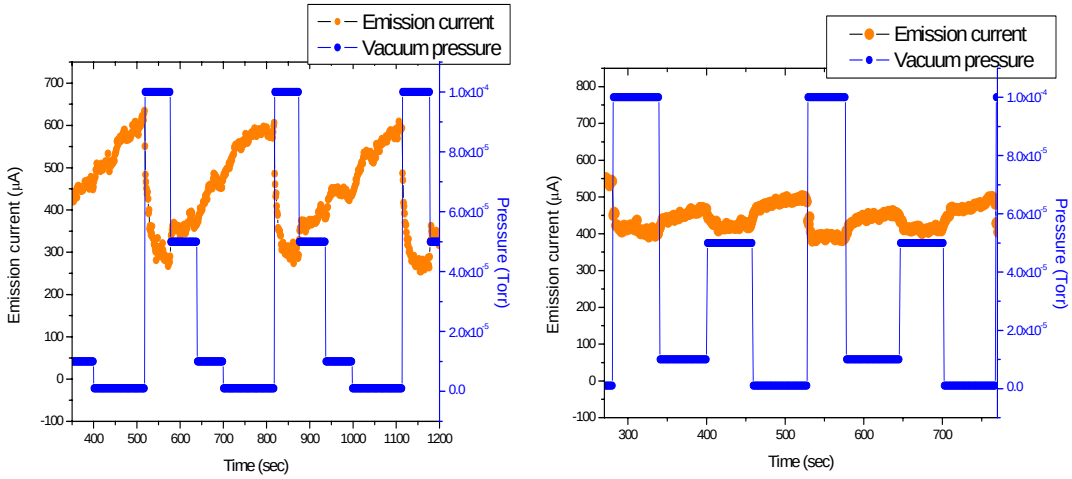

(a) (b)

Figure 3 Dynamic field emission currents of CNTs measured with changing pressures under (a) nitrogen and (b) argon.

(2) High-sensitivity molecule sensors using arrayed Si nanotips

As schematically illustrated in Figure 4, the use of nanotips as supports for self-assembly of gold and silver nanoparticles can be much more effective in SERS due to their high-density of "hot spots", namely, closely spaced metal nanoparticles which are SERS active sites. A particle density close to the case of particles touching each other under a monolayer coverage is required that can be easily achieved by tuning the sputtering time. A low sputtering time, say 1 min, produced nanoparticles near the apex of the tips. As the sputtering time increased, the density of nanoparticles increased across the surface of the nanotip. A maximum density was obtained for a sputtering time of 10 min for the particular IBS configuration used, after which agglomeration of the particles were observed resulting in a uniform thin film of silver. The distribution of Ag nanoparticles on SiNTs is shown in Figure 5 as a function of the sputtering time.

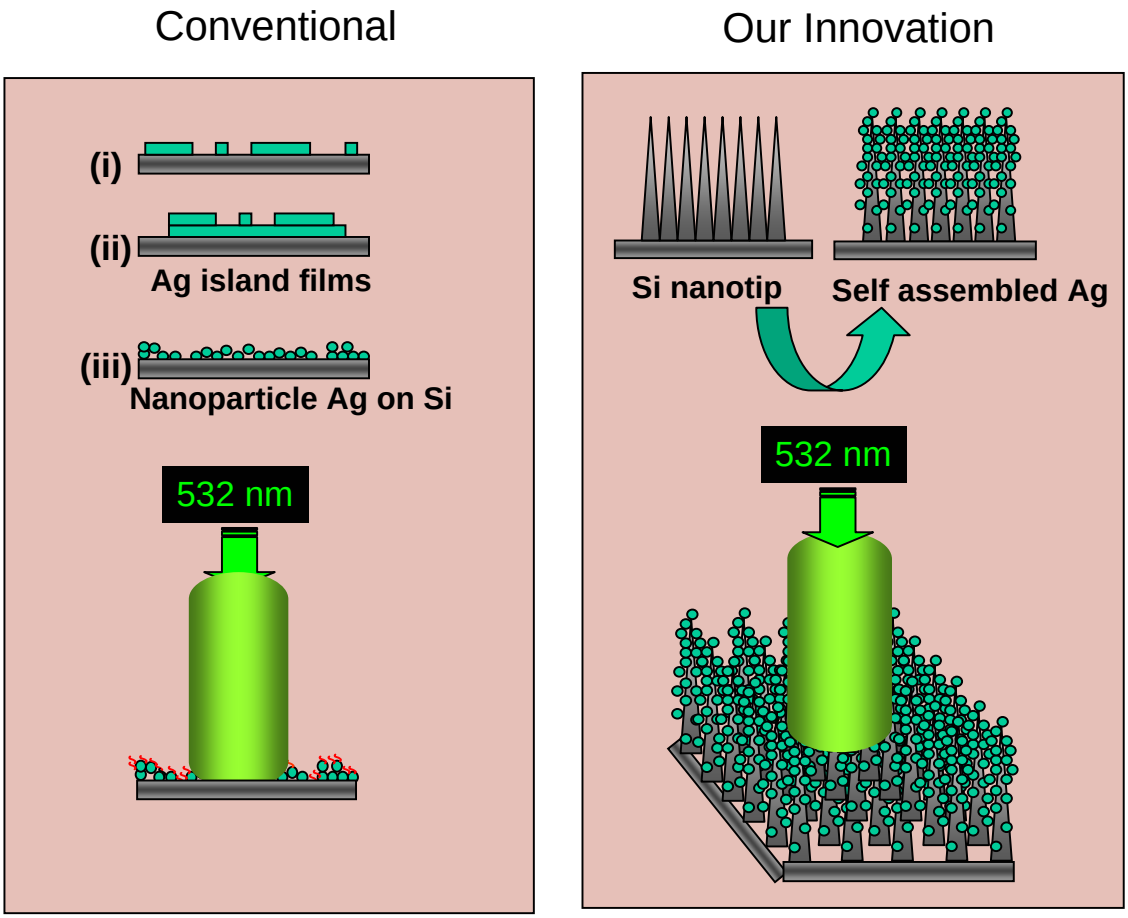

Figure 4 Schematic illustration of how using SiNTs as a template for depositing Ag nanoparticles can provide high-density "hot spots" for SERS.

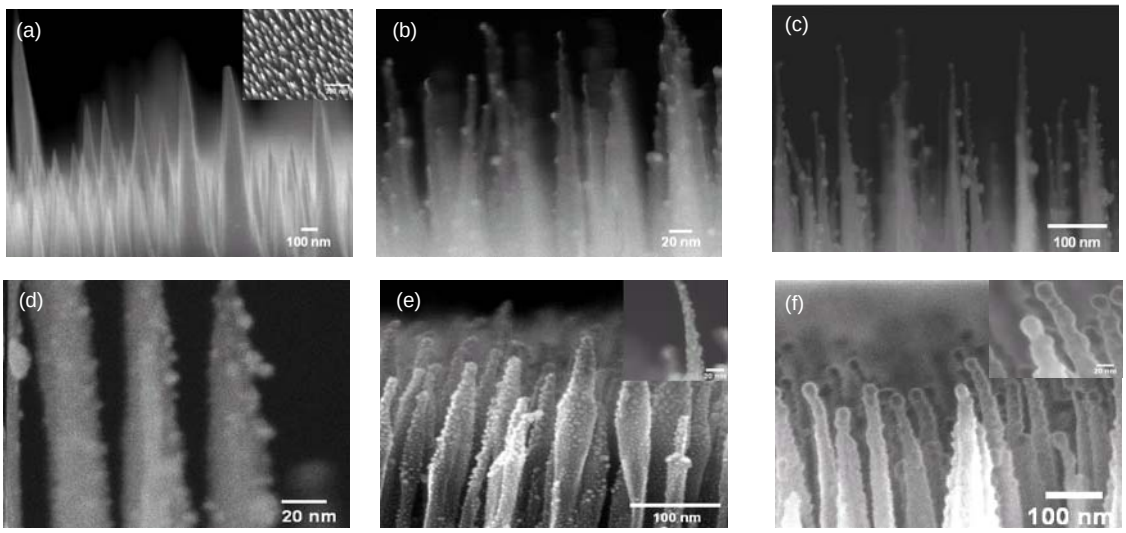

Figure 5 SEM micrographs showing (a) cross-sectional view of the as-grown SiNTs (inset shows the top view); cross-sectional images of SiNTs covered with Ag sputtered for (b) 1 min, (c) 3 min, (d) 5 min, (e) 10 min, and (f) 20 min in IBS (insets in e and f are the magnified images).

These Ag-coated SiNTs are SERS active substrates. Even low concentrations (10^{-6} to 10^{-10} M) of molecules, such as Rhodamine 6G (R6G) and bis-pyridyl ethylene (BPE), can be detected by the SERS technique. As shown in Figure 6, the SiNTs coated by 10 min of sputtered Ag (Figure 5e) produced the best enhancements, as expected, because it possessed the necessary size and density of the metal nanoparticles. Enhancements in the range of 10^5 to 10^8 were observed with low concentrations of R6G and BPE.

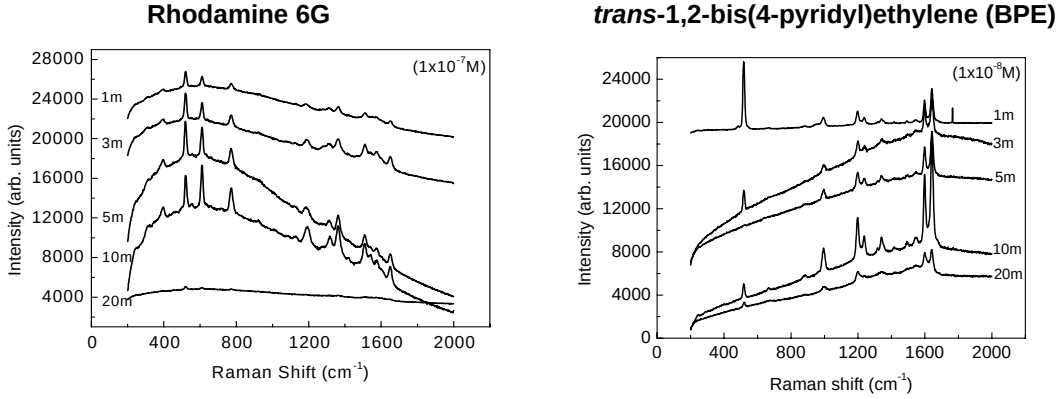

Figure 6 SERS spectra of R6G (10^{-7} M) and BPE (10^{-8} M) adsorbed on SiNTs coated with Ag nanoparticles with particle density.

Wetting properties measured for a series of SiNTs, which were fabricated at different substrate temperatures and their length was found to vary inversely with the substrate temperature, are shown in Figure 7. It should be emphasized here that a single parameter tunability of the length of the SiNT, and hence the aspect ratio, α, has been achieved by simply varying the process temperature. Similarly, inter-particle distance, β, can be controlled by the gas flow ratios. A higher Ar/H_2 and lower SiH_4/CH_4 will increase β, and vice versa. Figures 8(a) and 8(b) show the advancing (θ_{adv}) and receding (θ_{rec}) water contact angles as a function of α and β, respectively. For the high α or β case only θ_{act} is shown, since θ_{adv} and θ_{rec} could not be measured due to the superhydrophilicity demonstrated in them. θ_{act} is the intrinsic water contact angle measured with a horizontal substrate and fixed droplet volume.

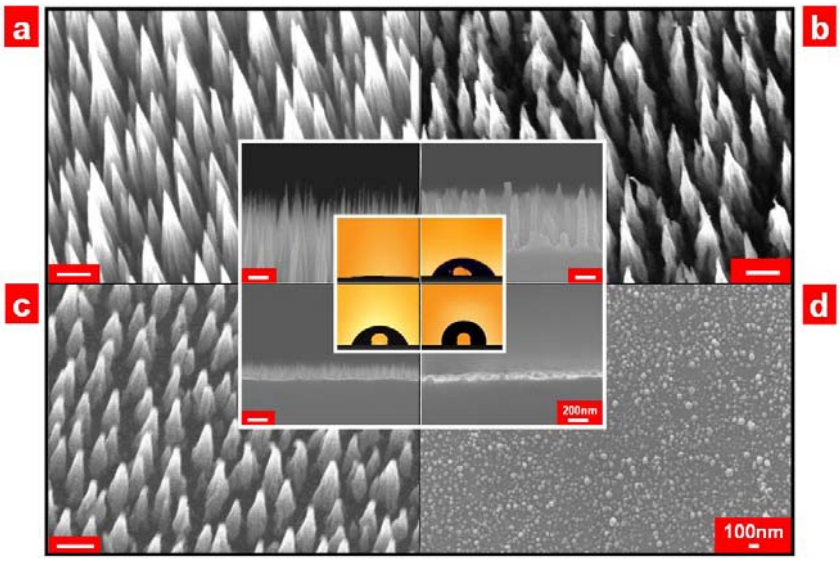

Figure 7 Tilted view SEM images of SiNTs grown at different temperatures: (a) 250 ˚C. (b) 400 ˚C. (c) 600 ˚C and (d) 700 ˚C. The inset shows the cross-sectional SEM image and the corresponding optical photograph of a water droplet indicating the contact angle.

Measurements of the water contact angle (θ) performed on SiNTs having different α yielded a very interesting result. A systematic decrease in θ has been observed with increasing α and can reproducibly approach 2˚ at large α (~ 15). The larger α (>12)

showed super-hydrophilicity (θ_{act} ~ 2˚), whereas the smaller α (<5) progressively showed lesser hydrophilicity (increasing θ_{act}), as shown in Figure 8(a), wherein the inter-tip distance (β) was kept between 100 and 180 nm. The samples with α = 2, 3, had β on the larger side. It is understood that surface energy and adhesion tension that dictate the wetting properties of a solid surface will vary as a function of the roughness of the surface. The variation of θ as a function of β, measured for very long (7 μm) and short (250 nm) SiNTs is shown in Figure 8(b). Interestingly, θ decreased for the shorter SiNTs and increased for the longer ones, and β was increased. For the shorter as well as longer SiNTs, a large β ($l/\beta < 1$) implies a morphology close to an intrinsic flat silicon surface, hence $\theta_{act} \approx 48^{\circ}$. An increasing roughness instilled by a small β should then drive the surface to hydrophilicity, which it does for the longer SiNTs. However, for the shorter SiNTs the trend is that of an increasing θ, although θ_{rec} stays close to the intrinsic value for flat Si. The results of increasing θ for the low α and β (shorter SiNTs) have been repeated and are reproducible.

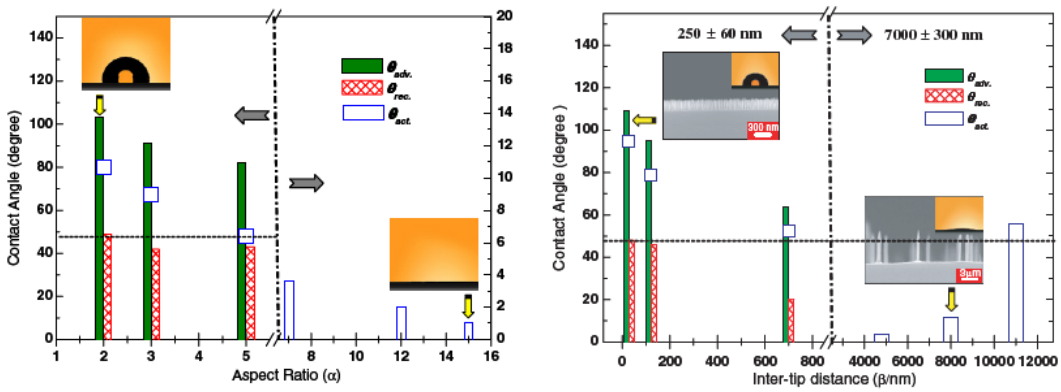

(a) (b)

Figure 8 Advancing, receding and intrinsic water contact angles as a function of (a) aspect ratios α, and (b) inter-tip distance β of the SiNTs. The optical photograph of a water droplet indicating the contact angle is shown for two different α and β values. A reference value of the water contact angle at 48˚ for a polished silicon wafer is indicated by the dashed line.

The wetting property of the SiNTs can be altered further by chemical modification. Consider SiNTs with a high value of α that yields vanishing water contact angles. Then the same SiNTs were modified using Ar ion-beam sputtering of a TiO_2 target. The TiO_2 formed particle-like features on the SiNTs. In contrast, a similar coating of TiO_2 on a polished Si wafer produced $\theta_{act} \approx 72^\circ$. The amphiphilic (hydrophilic as well as oleophilic) TiO_2 shows super-hydrophilicity when irradiated by UV light. However, in our case, when deposited on the SiNTs they exhibited hydrophobicity. Upon coating with TiO_2, the superhydrophilic SiNT with $\theta_{act} \approx 2^\circ$ (figure 7(a)) exhibits $\theta_{act} \approx 140^\circ$ with $\theta_{rec} = 74^\circ$ and $\theta_{adv} = 110^\circ$. Assuming a similar roughness for the bare SiNTs and those coated with TiO_2, switching from wetting to de-wetting behaviour has been observed with the help of a TiO_2 layer.

Conclusion

On-chip direct growth approach has been successfully applied to fabricate miniaturized field emission gas sensors. Field emission of CNTs operated under different ambient pressures of nitrogen and argon shows distinguishable characteristic electrical signals. In general, CNTs field emission sensors can be applied to test pressures below 10^{-4} Torr. The CNTs emitters also show higher sensitivity to nitrogen than to argon. However, the recovery and response time is shorter for argon than for nitrogen.

Self assembled Au and Ag nanoparticles monodispersed on SiNTs etched out of crystalline silicon substrates demonstrate high activity for surface enhanced Raman scattering. These macroscopic substrates possess the attributes such as uniform particle size (4-10 nm), controllable interparticle distance, and large enhancement factors (10^5-10^8). The high density of the SiNTs ($10^{11}/cm^2$) and a consequent uniform density of the metal nanoparticles, which can be controlled by the ion beam sputtering time of the metal targets, ensures high levels of inter and intra-substrate reproducibility. Molecules with concentrations as low as 10^{-10} M could be detected in a reproducible and stable fashion with the help of these substrates. The wetting properties of SiNTs have also been studied. By controlling the morphology of the nanotips, namely their length and density, the hydrophilicity of the SiNTs can be reproducibly tailored. Super-hydrophilicity has been

achieved for nanotips with a high aspect ratio. An unusual switching of the wetting properties has been observed upon chemical modification of the surface of the nanotip by coating with TiO_2 that renders it hydrophobic. These substrates can be useful systems for fundamental modeling as well as analytical tools for defense applications.

References

[1] L. C. Chen, C. Y. Wen, C. H. Liang, W. K. Hong, K. J. Chen, H. C. Cheng, C. S. Shen, C. T. Wu and K. H. Chen, *Adv. Func. Mater. 12* (2002) 687.

[2] C. P. Juan, K. J. Chen, C. C. Tsai, K. C. Lin, W. K. Hong, C. Y. Hsieh, W. P. Wang, R. L. Lai, K. H. Chen, L. C. Chen and H. C. Cheng, *Jpn. J. Appl. Phys. 44* (2005) 365.

[3] H. C. Cheng, W. K. Hong, F. G. Tarntair, K. J. Chen, C. P. Lin, K. H. Chen and L. C. Chen, *Electrochemical and Solid-State Lett. 4* (2001) H5.

[4] W. K. Hong, K. H. Chen, L. C. Chen, F. G. Tarntair, K. J. Chen, C. P. Lin and H. C. Cheng, *Jpn. J. Appl. Phys. 40* (2001) 3468.

[5] K. J. Chen, W. K. Hong, C. P. Lin, K. H. Chen, L. C. Chen and H. C. Cheng, *IEEE Electron Device Lett. 22* (2001) 516.

[6] H. C. Lo, D. Das, J. S. Hwang, K. H. Chen, C. H. Hsu, C. F. Chen and L. C. Chen, *Appl. Phys. Lett. 83* (2003) 1420.

[7] C. S. Chang, S. Chattopadhyay, L. C. Chen, K. H. Chen, C. W. Chen, Y. F. Chen, R. Collazo and Z. Sitar, *Phys. Rev. B 68* (2003) 125322.

[8] S. C. Shi, C. F. Chen, S. Chattopadhyay, K. H. Chen and L. C. Chen, *Appl. Phys. Lett. 87* (2005) Art. No. 073109.

[9] C. P. Juan, C. C. Tsai, K. H. Chen, L. C. Chen and H. C. Cheng, *Jpn. J. Appl. Phys. 44* (2005) 2612.

[10] J. Kong, N. R. Franklin, C. Zhou, M. G. Chapline, S. Peng, K. Cho and H. Dai, *Science 287* (2000) 622.

[11] P. G. Collins, K. Bradley, M. Ishigami, A. Zettl, *Science 287* (2000) 5459.

[12] J. Zhao, A. Buldem, J. Han and J. P. Lu, *Nanotechnology 13* (2002) 19.

[13] A. Modi, N. Koratkar, E. Lass, B. Wei and P. M. Ajayan, *Nature 424* (2003) 171.

[14] S. Chattopadhyay, H. C. Lo, C. H. Hsu, L. C. Chen and K. H. Chen, *Chem. of Mater. 17* (2005) 553.

[15] S. Chattopadhyay, S. C. Shi, Z. H. Lan, C. F. Chen, K. H. Chen and L. C. Chen, *J. Am. Chem. Soc. 127* (2005) 2820.

[16] H. C. Lo, Y. F. Huang, S. Chattopadhyay, C. H. Hsu, C. F. Chen, K. H. Chen and L. C. Chen, *Nanotechnology 17* (2006) 2542.

[17] C. H. Hsu, C. F. Chen, H. C. Lo, D. Das, J. Tsai, J. S. Hwang, L. C. Chen and K. H. Chen, *Nano Lett. 4* (2004) 471.

[18] K. H. Chen, J. S. Hwang, H. C. Lo, D. Das and L. C. Chen, U. S. Patent 6,960,528 B2, Nov. 1 (2005).

Project Related Activities

During this work period, I have made a second technical visit to AFRL Hanscom in November 7-8, 2005. My AFRL visit was arranged by Dr. Yu-Hui Chiu at Hanscom AFB with Dr. Michael Alexander as the co-host. The opportunities of discussing the actual works pursued and needs at Hanscom AFRL and person-to-person discussion on the relevant technical issues are indeed valuable. Detail of this visit has been described in a separate WOS trip report. Frequent interaction with Dr. Yu-Hui Chiu has been continued till now. Ideas about joint efforts have also been exchanged. In fact, some CNTs specimens made in our lab were sent to Hanscom for testing and we have also received some tungsten samples from Dr. Chiu for further nano-engineering and surface treatment. Preliminary results of our studies on tungsten are shown as supplementary information in a separate file.

Appendix I: Selective Project Related Publications

(1) 'Morphology Control of Si Nanotips Fabricated by Electron Cyclotron Resonance Plasma Etching', C. H. Hsu, Y. F. Huang, L. C. Chen, S. Chattopadhyay, K. H. Chen, H. C. Lo and C. F. Chen, *J. Vac. Sci. Technol. B 24*, 308 (2006).
[AFOSR support explicitly indicated]

(2) 'Nanotips: Growth, Model and Applications', S. Chattopadhyay, L. C. Chen and K. H. Chen, *Critical Reviews in Solid state and Material Science 31*, 15-53 (2006).
[AFOSR support explicitly indicated]

(3) 'Geometrically Tuned and Chemically Switched Wetting Properties of Silicon Nanotips', H. C. Lo, Y. F. Huang, S. Chattopadhyay, C. H. Hsu, C. F. Chen, K. H. Chen and L. C. Chen, *Nanotechnology 17*, 2542 (2006).
[AFOSR support explicitly indicated]

(4) 'Surface Enhanced Raman Spectroscopy Using Self Assembled Silver Nanoparticulates on Silicon Nanotips', S. Chattopadhyay, H. C. Lo, C. H. Hsu, L. C. Chen and K. H. Chen, *Chem. of Mater. 17*, 553 (2005).

(5) 'Molecular Sensing with Ultrafine Silver Crystals on Hexagonal Aluminum Nitride Nanorod Template', Surojit Chattopadhyay, Shi Chen Shi, Zon Huang Lan, Chia Fu Chen, Kuei-Hsien Chen and Li-Chyong Chen, *J. Am. Chem. Soc. 127*, 2820 (2005).

(6) 'Improved Field Emission Properties of Carbon Nanotube Field-Emission Arrays by Controlled Density Growth of Carbon Nanotubes', C. P. Juan, K. J. Chen, C. C. Tsai, K. C. Lin, W. K. Hong, C. Y. Hsieh, W. P. Wang, R. L. Lai, K. H. Chen, L. C. Chen and H. C. Cheng, *Jpn. J. Appl. Phys. 44*, 365 (2005).

(7) 'Fabrication and Characterization of Lateral Field Emission Device Based on Carbon Nanotubes', C. P. Juan, C. C. Tsai, K. H. Chen, L. C. Chen and H. C. Cheng, *Jpn. J. Appl. Phys. 44*, 2612 (2005).

(8) 'Effects of High-density Oxygen Plasma Post-treatment on Field Emission Properties of Carbon Nanotube Field-emission Displays', C. P. Juan, C. C. Tsai, K. H. Chen, L. C. Chen and H. C. Cheng, *Jpn. J. Appl. Phys. 44*, 8231 (2005).

Appendix II: Selective Project Related Invited Talks at International Conferences

(1) SPIE-Optics East (Oct. 1-4, 2006), Symposium PT103: Nanostructure Integration Techniques for Devices, Circuits and Systems: Interfaces, Interconnects and Nanosystems II, on *"Functional one-dimensional nanostructures as photoconductor, molecular sensor and wavelength-selective nanoswitch"*, Boston, MA, USA
[AFOSR support explicitly acknowledged]

(2) 11th International Ceramics Congress and 4th Forum on New Materials (CIMTEC, June 4-9, 2006), on *"Ultrafine nanoparticles uniformly dispersed on arrayed CNTs for energy applications"*, Sicily, Italy

[AFOSR support explicitly acknowledged]

(3) International Conference on Nano Science and Technology (ICONSAT, March 16-18, 2006), on "*One-dimensional nanostructures: from lasing to sensing*", New Delhi, India

[AFOSR support explicitly acknowledged]

(4) 2005 MRS-Fall Meeting (Nov. 28-Dec.2, 2005), Symposium R: Assembly at the Nanoscale, on *"Functionalization of nanotips: from field emission, antireflection to molecular sensing devices"*, Boston, MA, USA

[AFOSR support explicitly acknowledged]

(5) China Nano 2005 (June 9-11, 2005), China International Conference on Nanoscience & Technology, on *"Field emission, antireflection and molecule/particle sensing devices based on arrayed nanotips"*, Beijing, China

[AFOSR support explicitly acknowledged]

Fabrication and Characterization of Sharp Tungsten Tip

Objectives:

To improve the performance of the thruster fuel injector, a focused research has been carried out to sharpen the tungsten tips to nanoscale and modify the surface of tungsten for optimized wetting properties.

Executive Summary:

Sharp and smooth tungsten tips (nanoscale) have been successfully fabricated from tungsten wires by electro-chemical etching with scanning-and-holding lifting speeds during the etching process. The same technique has also been applied to reduce the diameter of the tungsten tips supplied by AFRL from microscale to nanoscale. However, ECR plasma using gas mixture of methane, silane, hydrogen and argon is not adequate (or efficient) to etch tungsten. Fluorine-containing gases are suggested for future experiments. The wetting property of tungsten subjected to various surface treatments is relatively stable against EMIMIm / $C_8H_{11}F_6N_3O_4S_2$, an ionic liquid for thruster, as compared to DI water.

Two methods were tried for nanoscale engineering of tungsten: (i) Electro-chemical etching of tungsten wires and micro-tips, and (ii) Electron cyclotron resonance (ECR) plasma-etching of tungsten surface. The scheme of electro-chemical etching process of the tungsten wire/tip is shown in figure 1(a). Etching experiment was typically performed in KOH at 6 Volts. The reactions occurred during electro-chemical etching are shown below:

Anode reaction: $W_{(s)} + 8OH^-_{(aq)} \rightarrow WO^{2-}_{4\ (aq)} + 4H_2O + 6e^-$

Cathode reaction: $2H_2O + 2e^- \rightarrow H_{2(g)} + 2OH^-_{(aq)}$

Net reaction: $W_{(s)} + 2H_2O + 2OH^-_{(aq)} \rightarrow WO^{2-}_{4\ (aq)} + 3H_{2(g)}$

The shape of tungsten tip can be controlled with different lifting speed of the tungsten wire, as schematically illustrated in figure 1(b).

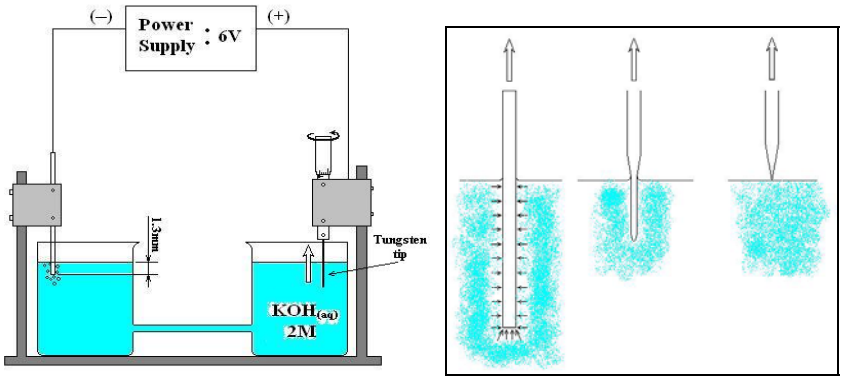

(a) (b)

Figure 1 (a) The schematic diagram of electro-chemical etching process for tungsten tips. (b) Tip shape evolution by electro-chemical etching with different lifting speeds.

Two different speed lifting procedures, namely, at a constant speed (0.1 mm/min) and with a scanning-and-holding program of speeds (from 0.1 mm/min gradually increased to 0.5 mm/min), have been utilized to fabricate the tungsten tips, and the resultant morphologies are shown in figures 2 and 3, respectively. When a constant

lifting speed was utilized, a contracted edge with a neck-like morphology of the tungsten tip is clearly visible (Fig. 2). In contrast, the scanning-and-holding approach allows us to eliminate the neck formation, resulting in uniform tungsten tip (Fig. 3).

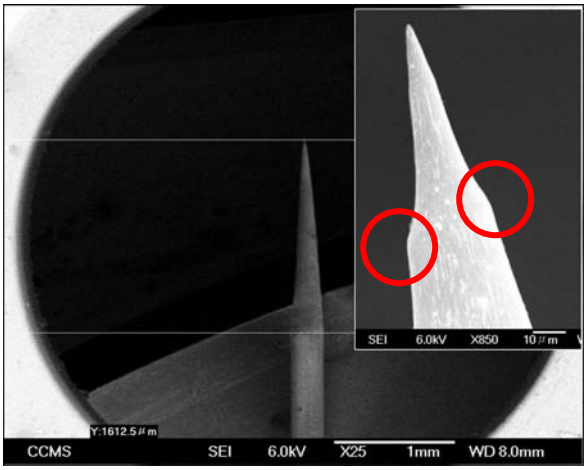

Figure 2 Neck morphology is observed on the etching sidewall of the tungsten tip using constant lifting speed at 0.1 mm/min.

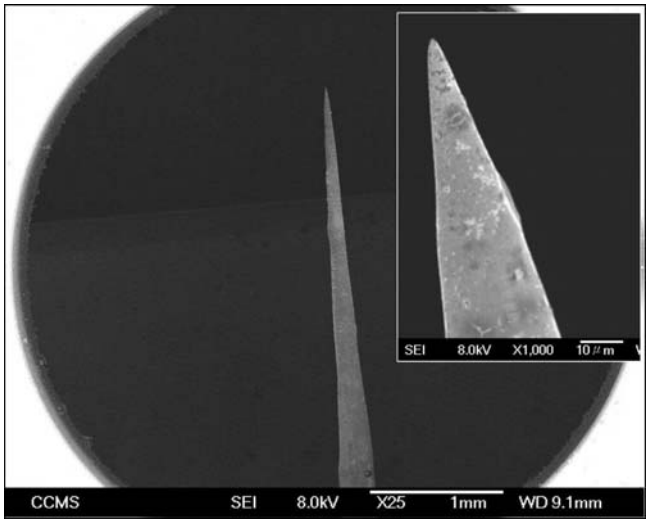

Figure 3 When produced by varying lifting speeds from 0.1 to 0.5 mm/min, tungsten tip shows a smoothly tapered etching sidewall.

Based on these results, the second procedure, i.e., with varying lifting speeds, is thus established as the standard practice for the electrochemical etching of tungsten. Two sets of tungsten samples (which were provided by Dr. Yu-Hui Chiu from the Air Force Research Lab located in Hanscom AFB, MA) having different diameters and initial

tip shapes have been evaluated. All the as-received samples have “fatty tips”, i.e., they have high apex angles and low tip height-to-base diameter ratios. As shown in figure 4: (a) and (b) are the SEM images of the fatty tungsten tips with a blunt tip diameter > 10 μm; (c) and (d) are the corresponding SEM images of the tips after electrochemical etching. The other set had an initially sharper tip with tip diameter < 10 μm. The corresponding SEM images of the tips before and after etching are shown in figure 5.

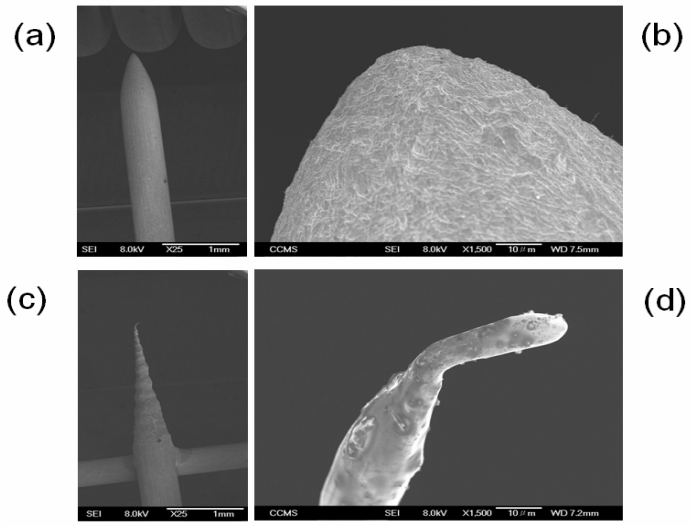

Figure 4 The SEM images of (a) & (b) as-received “blunt” tungsten tips from AFRL, and (c) & (d) after electrochemical etching.

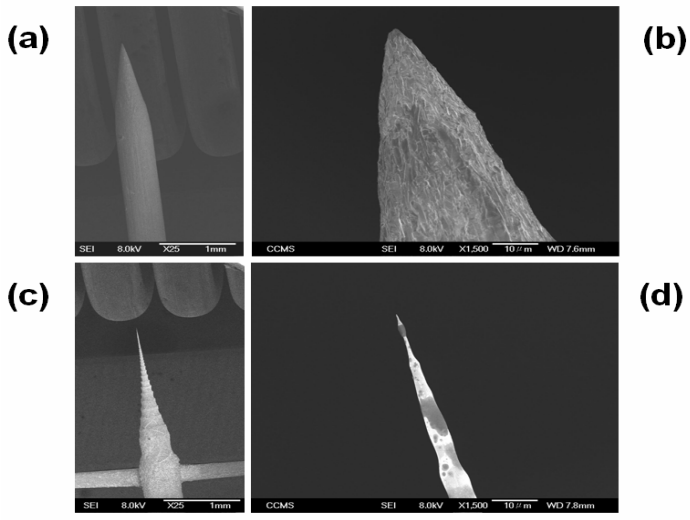

Figure 5 The SEM images of (a) & (b) as-received “sharp” tungsten tips from AFRL, and (c) & (d) after electrochemical etching.

While significant reduction in the apex angle and tip diameter has been achieved by electrochemical etching of the tungsten tips provided by AFRL, the optimized tip morphology is obtained by electrochemical etching directly from tungsten wire using the procedure established at NTU.

Alternatively, we have employed high-density electron cyclotron resonance (ECR) plasma process using gas mixtures of silane, methane, argon, and hydrogen to modify the surface of tungsten foils and wires. The ECR process was developed at NTU and has been patented as a one-step process for producing high-density arrayed nanotips over large area. This process has been successfully applied to a wide range of materials, including Si, GaAs, GaN, sapphire, Cu and Al. However, it is quite difficult to produce tungsten nanotips by ECR process with the aforementioned gas mixtures. As shown in figure 6, no obvious difference can be seen after 6 hours of ECR etching.

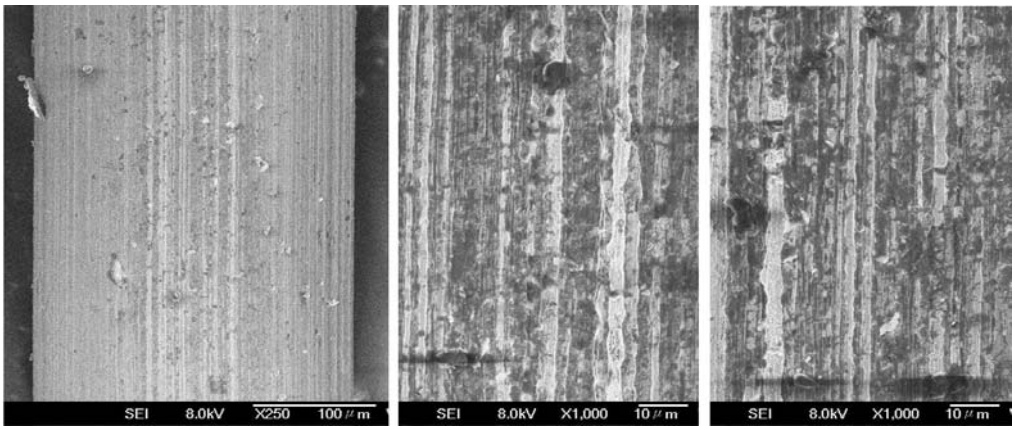

(a) (b) (c)

Figure 6 The SEM images of tungsten tip (a) sidewall of tungsten tip before etching (low resolution) (b) sidewall of tungsten tip (high resolution) (c) after ECR plasma etching for 6 hours using gas mixtures of silane, methane, argon, and hydrogen.

It is known that fluorine-containing gases, in particular, SF_6, CF_4, and NF_3, should provide more efficient etching using conventional reactive ion etching (RIE) process. Etching rates as high as 100 nm/min and good uniformity of etched tungsten materials

have been reported using SF_6 /Ar, CF_4 / Ar or NF_3/O_2 plasma at low pressure environment in literature. However, these gases are more corrosive and a separate reactor will be required for such experiments.

Meanwhile we have investigated the wetting property, via surface contact angle measurement, of the tungsten foil surface treated with different plasma. Two types of liquids, DI water and ionic liquid (EMIMIm / $C_8H_{11}F_6N_3O_4S_2$), of which the latter one is used for the thruster, have been tested. The contact angle of the DI water and the ionic liquid on tungsten foil without any surface treatment is quite similar, about 67°. After 30-min of hydrogen and ammonia plasma treatment, the contact angle of the DI water on W increased by more than 10° while negligible change in contact angle of the ionic liquid was observed (figure 7).

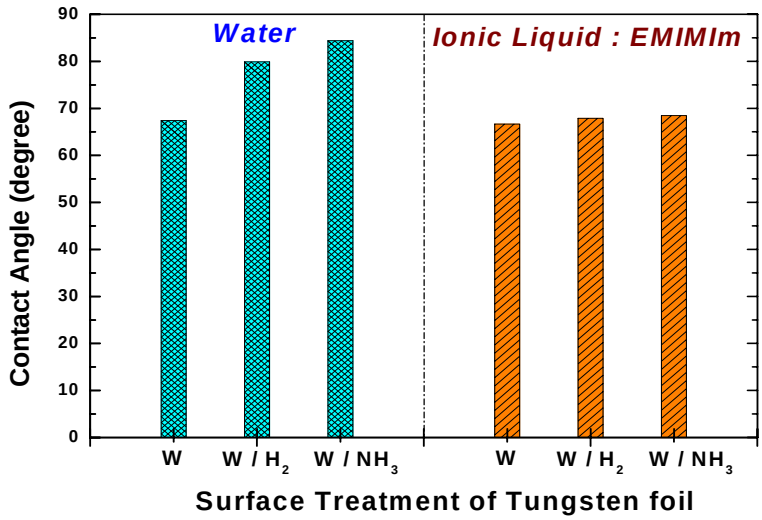

Figure 7 The contact angle of DI water and an ion liquid on tungsten foil with various surface treatments.